Energy-Transfer Study of Cytochrome b_5 Using the Anthroyloxy Fatty Acid Membrane Probes†

Alan M. Kleinfeld* and Michael F. Lukacovic‡

Biophysical Laboratory, Department of Physiology and Biophysics, Harvard Medical School, Boston, Massachusetts 02115

Received June 12, 1984

ABSTRACT: Resonance energy transfer was used to study the structure of cytochrome b_5 and its nonpolar segment reconstituted into sonicated vesicles of dimyristoylphosphatidylcholine. The *n*-(9-anthroyloxy) (AO) fatty acid probes were added to these vesicles, and energy-transfer measurements were carried out between tryptophan and AO, tryptophan and the heme moiety of cytochrome b_5, and AO and heme. Results of these measurements were analyzed by using the methods outlined in the previous paper [Kleinfeld, A. M. (1985) *Biochemistry* (preceding paper in this issue)]. We find, in agreement with Fleming et al. [Fleming, P. J., Koppel, D. E., Lau, A. L. Y., & Strittmatter, P. (1979) *Biochemistry 18*, 5458–5464], that the fluorescent tryptophan in both forms of the protein is buried about 20 Å from the surface and that most of the fluorescence is associated with a single tryptophan. The results are consistent with the AO probe distance of closest approach to the protein, greater for whole b_5 than for the nonpolar peptide. The tryptophan–heme and AO–heme measurements indicate that the heme moiety is about 15 Å from the surface of the membrane. The agreement of our results with the previous studies supports the description of tryptophan–AO energy transfer outlined in the preceding paper.

Cytochrome b_5 serves as a vital link in the electron transfer processes on the surface of endoplasmic reticulum. Structural information at the molecular level is a necessary prerequisite for understanding this mechanism. A number of studies indicate that the protein is composed of a heme containing polar segment located above the plane of the membrane and a nonpolar segment buried half-way into the membrane (Dailey & Strittmatter, 1981). A 2.8-Å image of the polar segment, obtained by X-ray diffraction, reveals an approximately 40 Å long cylinder with the heme moiety located in what is probably an aqueous pocket (Mathews et al., 1979). From biochemical studies, the nonpolar peptide (NPP) of the protein appears to loop once into the bilayer, so that the N and C termini are both exposed on the outer surface (Dailey & Strittmatter, 1981). The primary structure predicts that tryptophan residues are in the loop, and fluorescence quenching studies demonstrate that they are buried in the membrane (Leto & Holloway, 1979). Resonance energy transfer between tryptophan and two acceptor molecules on the surface has shown that the fluorescent tryptophan is located at the center of the bilayer (Fleming et al., 1979).

To extend the molecular picture of the protein and to use this well-characterized system to test the tryptophan–*n*-(9-anthroyloxy) (AO) energy-transfer method detailed in the previous paper (Kleinfeld, 1985), we have measured energy transfer between tryptophan and AO, tryptophan and heme, and AO and heme. These measurements were carried out in both the whole cytochrome b_5 and NPP, obtained from the whole protein by trypsin digestion. We find, in agreement with Fleming et al. (1979), that the fluorescent tryptophan in both forms of the protein is buried about 20 Å from the surface. The results from the heme-transfer measurements indicate that this moiety is about 15 Å from the surface of the membrane and thus in a reasonable position to serve in the electron-transfer process. It appears, therefore, that the essential features of the model of the previous paper (Kleinfeld, 1985) are correct, and it should be possible to use this approach for studying multi-tryptophan proteins.

Materials and Methods

Materials. Cytochrome b_5 purified from rabbit liver was a generous gift of Peter Holloway (University of Virginia, Charlottsville). Protein stock [88.5 μM in 20 mM tris(hydroxymethyl)aminomethane (Tris) and 50 mM NaCl, pH 7.4] was divided into 100-μL aliquots and stored at −20 °C. Dimyristoylphosphatidylcholine (DMPC) was purchased from Avanti and used without further purification. Small unilamellar vesicles were obtained by sonication for 1 h under N_2 at 28 °C. The suspension was centrifuged to remove titanium and large vesicles. Phospholipid concentration was determined by the Elon method (Gomori, 1942).

The *n*-(9-anthroyloxy) fatty acid probes (*n*-AO) [2-, 3-, 6-, 7-, 9-, 10-, and 12-(9-anthroyloxy)stearic acid (*n*-AS) and 16-(9-anthroyloxy)palmitic acid (16-AP)] were purchased from Molecular Probes. Probe purity was assessed by thin-layer chromatography in a solvent system of methanol–chloroform–hexane, 1:5:2 (Thulborn & Sawyer, 1978). Occasionally some samples exhibited impurities which ran at both higher and lower R_f values. In these cases the primary spot was purified by scraping the silica plate and eluting in ethanol. Stock solutions of the probes (0.5–5 mM) were prepared in ethanol and stored at −20 °C. Probe incorporation into vesicles was accomplished by addition of small volumes (<0.5% v/v) of the ethanolic solution to the vesicle suspension while rapidly vortex mixing. As monitored by fluorescence intensity, incorporation at room temperature was complete in less than 10 min.

Reconstitution. Protein–vesicle recombinants were formed by adding about 2 μM protein to a 200 μM phospholipid vesicle suspension. This suspension was incubated at 30 °C for 1 h, and incorporation of protein was monitored by observing the increase in tryptophan fluorescence, which reached

† This work was supported by Grant PCM-830268 from the National Science Foundation. This work was done during the tenure of an Established Investigatorship of the American Heart Association, and funds were contributed in part by the Massachusetts affiliate (82-174, to A.M.K.) and a Research Fellowship from the American Heart Association, Western Massachusetts Division (13-401-812, to M.F.L.).

‡ Present address: Sharon Woods Technical Center, The Procter and Gamble Co., Cincinnati, OH 45241.

0006-2960/85/0424-1883$01.50/0

a constant value after 30 min. Protein concentration was determined by heme absorption using an extinction coefficient at 412 nm of 1.5×10^5 $(M\ cm)^{-1}$.

The NPP fragment of the protein was prepared as described in Fleming & Strittmatter (1978). Following reconstitution of the whole cytochrome b_5 into DMPC, vesicles were incubated at 28 °C with 0.5 μg/mL trypsin for 1 h. This material was chromatographed on a Bio-Gel A-1.5 column (1 × 50 cm). To identify fractions containing reconstituted NPP, we measured the 90° scattering, tryptophan intensity, and heme absorption of the elution profile. The 90° scattering and tryptophan fluorescence yielded single, coincident peaks near the void volume and were well separated from the heme absorption peak which had no coincident tryptophan fluorescence.

Fluorescence Measurements and Analysis. Steady-state fluorescence measurements were performed on a Perkin-Elmer MPF-2A fluorometer modified for additional stability and interfaced to a PDP 11/34 computer (Kleinfeld et al., 1979). The fluorescence was measured in 3 × 3 mm or 10 × 10mm cuvettes. The fluorescence of a quinine sulfate solution in 0.1 N H_2SO_4 (excitation at 352 nm, emission between 380 and 600 nm) was recorded periodically throughout the course of an experiment (about 4 h) to monitor stability and to normalize the AO and tryptophan fluorescence. Uncertainties in the transfer efficiencies were estimated either from multiple determinations, from the difference in the values obtained from quenching and sensitized emission, or from the assumption that the intensity fluctuations of the quinine sulfate standard reflected the fluctuation of the tryptophan and AO intensities.

For studies on whole cytochrome b_5, experiments were carried out in two stages. In the first, AO probes were added to vesicles without protein, and the direct AO emission was determined by excitation at 290 and 383 nm. These measurements were used to determine the AO concentration and the ratio of the 290/383-nm contribution to the AO fluorescence. Protein was then added to these vesicles, and the 290- and 383-nm measurements were repeated to determine the tryptophan and AO intensities. These two steps were necessary since heme quenching interfered with the fluorescence determination of AO concentration. For NPP a single peptide–vesicle suspension was divided into 9 equal volumes. One of the AO probes or an equal volume of ethanol was added to each of the nine samples, and following probe incorporation fluorescence was measured by excitation at 290 and 383 nm.

Energy-transfer efficiencies (T) were determined from the quenching of tryptophan fluorescence according to

$$T = 1 - I/I^0 \tag{1}$$

in which I and I^0 are the tryptophan emission intensities in the presence and absence of AO probe. The intensities were evaluated by integrating the emission spectra between 310 and 400 nm and subtracting the scattering background. The scatter contribution, about 10% of the tryptophan intensity in samples without AO probe, was evaluated by using two methods which gave results in agreement with one another. In the first method emission intensities, following excitation at 290 nm, were measured with vesicles of the same lipid concentration as used to determine T, but without protein. In the second method, because of the uncertainties in the lipid concentrations and because protein incorporation might affect the scattering intensity, measurements were performed on protein-containing vesicles by making use of the negligible tryptophan absorption above 310 nm. The emission spectrum above 320 nm was determined following excitation at 290 nm. The spectrum was shifted −20 nm and multiplied by a factor equal to the ratio of the lamp intensities at 290 and 310 nm times the ratio of the excitation wavelengths to the 4th power (the Rayleigh scattering factor). Corrections were also made for the small (<1%) difference in self-absorption of samples with and without probe.

Transfer efficiencies were also determined from the intensity of sensitized emission. The fluorescence intensity in the region above 400 nm for excitation at 290 nm is given by

$$I = I_T + I_D + I_B + I_R \tag{2}$$

in which I_T is due to nonradiative transfer, I_D to direct emission, I_B to scattering and tryptophan background, and I_R to radiative migration.

The process in which AO fluorescence arises from the absorption of a photon is known as radiative migration. The magnitude of this process depends sensitively on the optical geometry and the AO concentration. Haigh et al. (1979) found that it was necessary to use front surface geometry to minimize this effect. In their study radiative migration resulted in significant fine structure in the tryptophan emission spectrum. In the Perkin-Elmer MPF-2A fluorometer, however, the major fraction of tryptophan photons responsible for AO emission originates from positions along the beam axis which are not visible to the collection optics. Thus, radiative migration, except for the relatively small contribution observed by the collection optics, cannot affect the tryptophan emission, and indeed, no significant spectral shape changes were observed upon addition of AO to the vesicles. On the other hand, we did observe a small increase in apparent sensitized emission when 10 × 10 mm cuvettes were used as compared to the 3 × 3 mm cuvettes. To determine if this effect was due to radiative transfer, a Monte Carlo calculation was performed to evaluate the intensity of AO fluorescence due to radiative transfer relative to the direct donor intensity. The results of this calculation demonstrated that the radiative migration contribution is 4–5 times smaller in 3 × 3 mm as compared to 10 × 10 mm cuvettes. Hence, the radiative transfer contribution may be ignored in measurements performed with the 3 × 3 mm cuvettes, and the transfer efficiencies obtained from the sensitized emission with the 10 × 10 mm cuvettes were not used.

The direct contribution was determined by measuring the ratio of AO fluorescence intensities at 290- and 383-nm excitation. This contribution is small for the AO probes since the absorption spectrum is at a local minimum in the 290–300-nm region. It was observed for all probes that $I_D = 0.011 I^{AO}(383)$, in which $I^{AO}(383)$ is the AO intensity observed by exciting the protein containing vesicles at 383 nm.

The intensity of sensitized emission due to energy transfer is given by

$$I_T = I^* Q_{AO}[1 - T(H)]T(AO) \tag{3}$$

in which I^* is the intensity of excited tryptophan, Q_{AO} the AO quantum yield, $T(H)$ the transfer efficiency from AO to heme, and $T(AO)$ is the transfer efficiency from tryptophan to AO. $T(H)$ is determined from the AO emission measured by exciting at 383 nm (direct excitation) and is zero for NPP. I^*, the intensity of excited tryptophan, can be expressed in terms of the measured tryptophan intensity (with no AO present) and the tryptophan quantum yield by

$$I^* = \frac{I^{Trp}}{Q_{Trp}} \tag{4}$$

The following expression for the tryptophan to AO transfer efficiency is obtained by substituting eq 3 and 4 into eq 2:

$$T(AO) = \frac{(I - I_B)Q_{Trp}}{I^{Trp} Q_{AO}[1 - T(H)]} \tag{5}$$

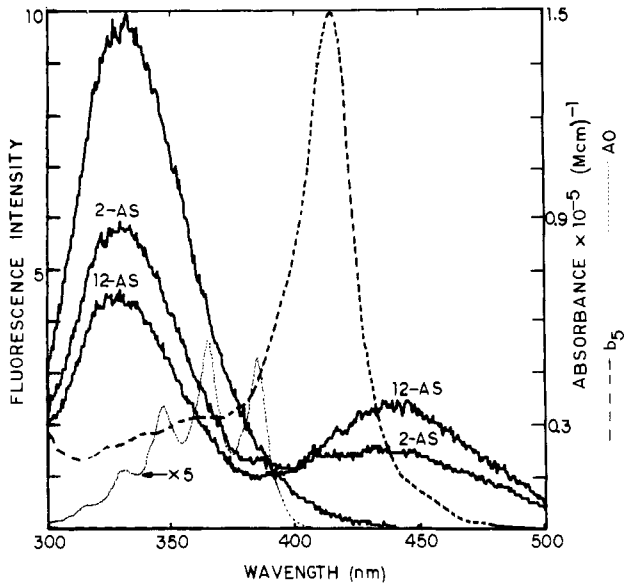

FIGURE 1: Fluorescence and absorption spectra in cytochrome b_5 vesicles. The fluorescence spectra (〰) were obtained by exciting DMPC vesicles containing whole b_5 at 290 nm. The most intense spectrum was obtained from vesicles unlabeled with AO probe and displays the emission characteristic of tryptophan. The two other fluorescence spectra were obtained from vesicles labeled with 2-AS and 12-AS at probe mole fractions (relative to phospholipid) of 2.5% and 2.2%, respectively. These latter spectra exhibit the reduced tryptophan and enhanced AO fluorescence characteristic of energy transfer between tryptophan and AO. Absorption of cytochrome b_5 and AO in vesicles was measured with a Cary 210 spectrophotometer.

Protein or AO surface densities (σ) were determined from their lipid phase concentrations $[X]_L$, the phospholipid concentration [PL], and the area/phospholipid molecule (A_L) according to

$$\sigma = \frac{1.54[X]_L}{[PL]A_L} \quad (6)$$

The factor of 1.54 results because the outer leaflet comprises 65% of these vesicles (Huang & Mason, 1978). A value of 70 Å^2 was used for A_L (Huang & Mason, 1978), and the area occupied by the probe or protein was neglected since their mole fraction was less than 3%. $[AO]_L$ was determined from its fluorescence intensity (excitation 383 nm) according to

$$[AO] = \frac{f(383/352)I(AO)[QS]\ Q_{QS}\epsilon_{QS}^{(352)}}{I(QS)Q_{AO}\epsilon_{AO}^{(383)}} \quad (7)$$

in which $f(383/352)$ is the ratio of exciting light intensity at 383 and 352 nm and $I(QS)$ is the fluorescence intensity of a quinine sulfate standard. The values used for the quinine sulfate quantum yield and extinction coefficient at 352 nm are 0.70 (Scott et al. 1970) and 5000 (M cm)$^{-1}$, respectively. The aqueous phase contribution to $I(AO)$ is negligible since the quantum yield in water is about 30-fold smaller than the lipid value, and virtually all the probe is membrane bound in these experiments.

Equation 7 modified for the appropriate excitation wavelengths was used to determine the tryptophan quantum yield by using the quantum yield of two standards and corrections due to tryptophan polarization (Shinitzky, 1972). The standards were L-tryptophan in water, $Q = 0.14$ (Eisinger, 1969), and quinine sulfate in 0.1 N H_2SO_4, $Q = 0.7$ (Scott et al., 1970).

RESULTS

Tryptophan–AO Energy Transfer. Energy-transfer efficiencies between tryptophan and AO were determined in DMPC vesicles reconstituted with whole cytochrome b_5 or NPP. Typical fluorescence emission spectra following excitation at 290 nm are shown in Figure 1. This figure illustrates that upon addition of AO probes to the reconstituted vesicles tryptophan intensity is quenched and a new peak appears at 440 nm. Most of the intensity at 440 nm is due to sensitized AO emission from resonance energy transfer, with other contributions (between 10 and 50% of the 440-nm intensity, depending upon probe) from direct excitation of AO at 290 nm and from radiative migration.

Energy-transfer efficiencies from tryptophan quenching and sensitized emission were obtained from these spectra by integrating intensities, applying corrections for direct excitation and using eq 1 and 5. The efficiencies determined from tryptophan quenching and sensitized emission were generally in excellent agreement (except in 10 × 10 mm cuvettes, as discussed under Materials and Methods), and we have, therefore, averaged these values. Efficiencies have been plotted as a function of Z_A (probe depth) and are shown in Figures 2 and 3. Errors (SD) were about 10% of the efficiencies except for T values below 0.2, in which case the uncertainty is greater. The patterns of efficiencies from both whole cytochrome b_5 and NPP are similar and display a monotonic increase of T with Z_A. For a given probe density, however,

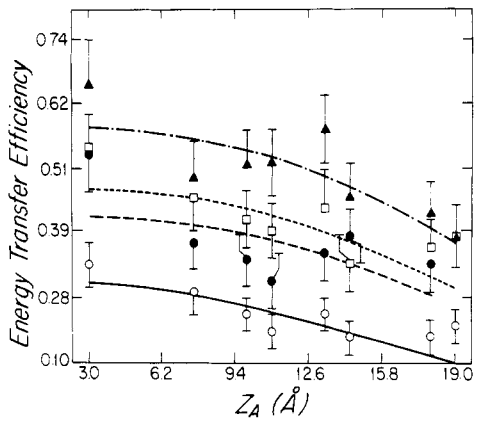

FIGURE 2: Energy-transfer efficiencies of whole cytochrome b_5. Energy-transfer efficiencies were measured at four different probe densities (in pmol/cm^2) and are plotted vs. the Z_A position of AO. The average probe densities for the four sets of measurements are (—) 7.2, (- - -) 9.0, (···) 12.0, and (-·-) 15.8. The lines through the experimental points are best single tryptophan fits for R_m = 18 Å and correspond to (y,z) values of about (10,1).

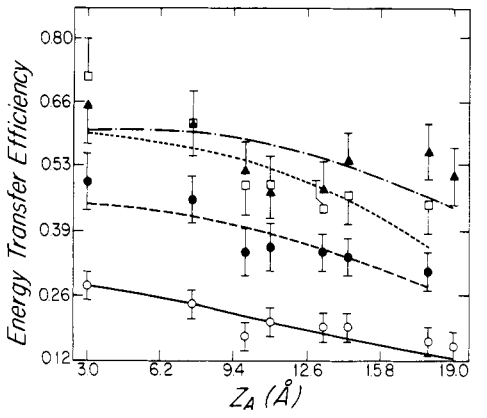

FIGURE 3: Energy-transfer efficiencies for NPP. Energy-transfer efficiencies were measured at four different probe densities (in pmol/cm^2) and are plotted vs. the Z_A position of AO. The average probe densities for the four sets of measurements are (—) 3.8, (- - -) 6.8, (···) 10.0, and (-·-) 10.6. The lines through the experimental points are best single tryptophan fits for R_m = 14 Å and correspond to y,z) values of about (8,–1).

Table I: Quantum Yields[a]

Trp NPP	Trp whole b_5	2-AS	3-AS	6-AS	7-AS	9-AS	10-AS	12-AS	16-AP
0.42	0.27	0.25	0.29	0.32	0.34	0.37	0.41	0.48	0.43

[a] The anthroyloxy quantum yields were determined in egg phosphatidylcholine vesicles relative to quinine sulfate ($Q = 0.7$). Uncertainties in these values (from multiple determinations) are approximately 10% for tryptophan and 5% for the AO probes.

the NPP transfer efficiency is greater than the value for whole b_5.

To control for possible aqueous phase contributions of protein fluorescence, energy-transfer measurements were carred out by adding the AO probes to an aqueous suspension of whole cytochrome b_5. The protein concentration was about the same as that used in the vesicle experiments (~ 2 μM), though the fluorescence intensity was about 30% that observed in the presence of vesicles (Leto & Holloway, 1979; Fleming et al., 1979). Addition of up to 20 μM AO had no effect on the tryptophan fluorescence, nor was the AO fluorescence affected by the protein's heme group. These results demonstrate that the contribution of unbound protein to the energy-transfer efficiency is negligible and, at least in buffer, there is no significant association between probe and protein.

The results shown in Figures 2 and 3 were analyzed by using the methods described in the previous paper (Kleinfeld, 1985). To perform this analysis, R_0 values (Table II) were determined by using the tryptophan Q values of Table I and the AO absorption spectrum of Figure 1. Both the shape and magnitude of the AO absorption spectra were found to be identical within experimental uncertainty (2%) for all the probes. Thus, if possible variations in K^2 and index of refraction (see below) are ignored, the R_0 values are identical for all the n-AO probes. The difference in R_0 values for whole b_5 (23.1 Å) and NPP (24.9 Å) is due to the smaller tryptophan Q value of whole b_5, which in turn is due to quenching by heme (see below).

A single tryptophan analysis was performed for each efficiency curve in Figure 2 and 3. Random tryptophan positions were chosen within a cylinder of length 80 Å (symmetric about the 40 Å wide bilayer) and varying radius. The analysis was performed for values of the radial parameter, R_m ($R_m = R_p$ + AO radius), between 8 and 22 Å. The corresponding energy-transfer efficiencies were calculated for each tryptophan position and were compared to the experimental curves by computing R^2 [eq 18 of Kleinfeld (1985)]. For each R_m value there is an optimum tryptophan location, and this corresponds to a minimum R^2 value, R^2_{min}. Among the R^2_{min} values for the various cylinders, there is a smallest value, or global minimum, R^2_G. The R_m dependence of the analysis is emphasized in Figures 4 and 5 by plotting R^2_{min}/R^2_G vs. R_m.

For the whole protein, as shown in Figure 4, R^2_{min}/R^2_G exhibits a precipitous drop in value between 12 and 18 Å and then rises very slightly for larger R_m. R^2_{min}/R^2_G values are large for R_m less than 18 Å because the distance of closest approach is small, and therefore, the calculated efficiencies are greater than the measured values. As R_m increases, the calculated T values decrease until around 18 Å where they provide a best fit to the experiment. Further increasing R_m results in only slightly smaller T values, since the fit increases the tryptophan y coordinate to maintain the same y–R_m separation as at 18 Å. Larger y values do, however, correspond to slightly different geometries, and therefore, the calculated T values are not identical with those for $R_m = 18$ Å. The results for the NPP (Figure 5) are similar to those of the whole protein except that the minimum R_m value occurs at about 14 Å, which also accounts for the increase in R^2_{min}/R^2_G with R_m observed in two of the measurements.

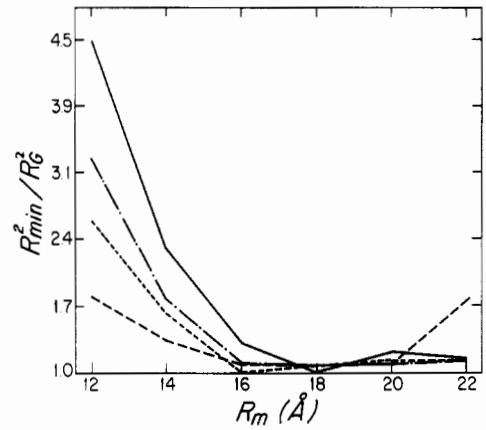

FIGURE 4: Radial dependence of energy transfer in whole b_5. The quantity R^2_{min}/R^2_G (explained in the text) is plotted vs. R_m, the energy-transfer radial parameter. The results of this single tryptophan analysis are shown for the four average probe densities of Figure 2, (—) 7.2, (- - -) 9.0, (···) 12.0, and (-·-) 15.8. The corresponding R^2_G values are 4.0, 8.2, 3.4, and 3.8.

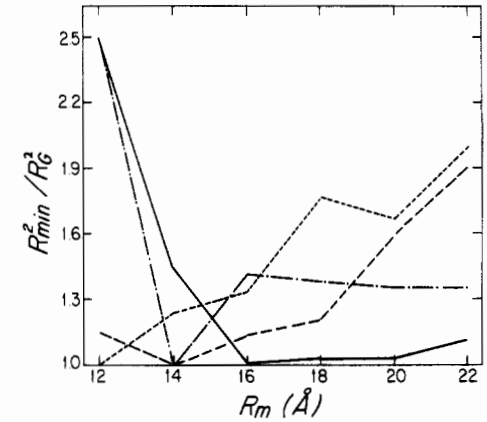

FIGURE 5: Radial dependence of energy transfer in NPP. The quantity R^2_{min}/R^2_G (explained in the text) is plotted vs. R_m, the energy-transfer radial parameter. The results of this single tryptophan analysis are shown for the four average probe densities of Figure 3, (—) 3.8, (- - -) 6.8, (···) 10.0, and (-·-) 10.6. The corresponding R^2_G values are 3.5, 3.3, 4.9, and 6.3.

These results indicate that the radial parameter is 14 ± 2 Å for NPP and 18 ± 2 Å for whole cytochrome b_5. With these values similar optimal y, z coordinates were obtained from all the efficiency curves. The average values, $y = 9 \pm 4$ Å and $z = -1 \pm 2$ Å, correspond to a single tryptophan located about 9 Å from the protein's axis and about 21 Å from the outer surface of the membrane. The calculated energy-transfer efficiencies corresponding to these optimal values have been plotted as lines in Figures 2 and 3. To illustrate the sensitivity of the measurement, one of the patterns of Figure 2 has been plotted in Figure 6 together with the patterns expected for a tryptophan shifted by 5–10 Å in the z and y directions, respectively. These results graphically demonstrate that shifts of this magnitude are incompatible with the measured efficiencies and also indicate the greater sensitivity in the z direction.

The measured energy-transfer efficiencies were also analyzed with two and three tryptophan, assuming equal quantum

Table II: R_0 Values (in Angstroms)[a]

	donor									
acceptor	Trp NPP	Trp whole b_5	2-AS	3-AS	6-AS	7-AS	9-AS	10-AS	12-AS	16-AP
AO	24.9	23.1								
heme (whole b_5)		29.3	36.3	37.0	37.7	38.2	38.6	39.2	40.2	38.4

[a] R_0 values were calculated by using the quantum yields of Table I and the absorption spectra of Figure 1.

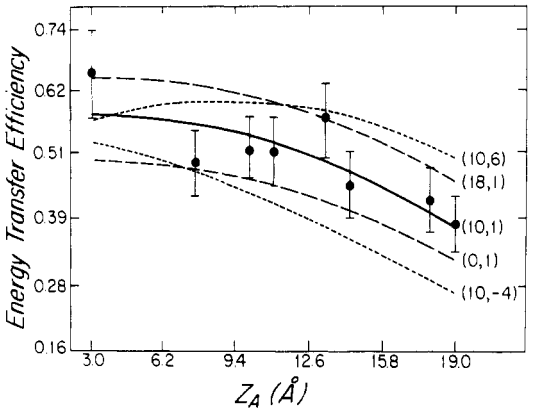

FIGURE 6: Tryptophan position sensitivity of energy-transfer efficiency. Data points are the whole b_5 results of Figure 2 for 15.8 pmol/cm^2, and the solid line through the data represents the best fit for a single tryptophan analysis. Energy-transfer efficiencies were calculated for positions which varied by ±5 Å in the z direction and +8 and −10 Å in the y direction. The (y,z) coordinates used for the calculations are shown to the right of each pattern.

yields for each tryptophan. Quantum yields were obtained by dividing the single value (Table I) by the number of tryptophan used in the analysis. The two tryptophan analysis of both whole protein and NPP displayed similar behavior. For virtually all the transfer efficiency curves the R^2_{min} occurred for R_m values less than or equal to 8 Å and was significantly greater than the value obtained in the single tryptophan analysis. The optimal y, z coordinates corresponded to two groups separated in the z direction by at least 10 Å, and for most of the curves the separation was greater than 16 Å. In the three tryptophan analysis R^2_{min} values were more than twice the single tryptophan values. The optimal coordinates from this analysis yielded a single tight cluster located near the center of the outer leaflet and squeezed onto the perimeter ($y \sim R_m$) of the cylinder.

Thus, two or more tryptophans with equal quantum yields provide a much poorer fit than a single tryptophan. In addition, the coordinates suggested from the two tryptophan fits are incompatible with the separation of tryptophan-108 and tryptophan-112 in an α helix (6 Å) or a β-pleated sheet (14 Å). The energy-transfer curves are, therefore, best fit with a single tryptophan analysis; consistent with most of the quantum yield concentrated in a single tryptophan, as suggested by Fleming et al. (1979).

Tryptophan–Heme Energy Transfer. Tryptophan quantum yields were determined by comparing the protein fluorescence with tryptophan and quinine sulfate standards as described under Materials and Methods. Assuming a single fluorescent tryptophan (Fleming & Strittmatter, 1978) for the whole protein and the nonpolar peptide, we obtained the results shown in Table I. The value for the NPP (0.42 ± 0.05) is significantly larger than the value found in whole protein (0.27 ± 0.04). We attribute this difference to energy-transfer quenching of the tryptophan by the heme moiety and not to structural differences in the two peptides since the tryptophan position is unaffected by the removal of the heme-containing portion. The quenching of the quantum yield corresponds to a transfer efficiency of 0.36 ($T = 1-Q_{whole}/Q_{NPP}$). Using $Q = 0.42$, $K^2 = {}^2/_3$, and the parameters listed in Table I, we obtain $R_0 = 29.3$ Å for tryptophan–heme transfer, and from $R = R_0(T^{-1} - 1)^{1/6}$, the tryptophan–heme separation is 32 ± 2 Å. Since this result is predicated on $K^2 = {}^2/_3$, it is subject to considerable error. In particular, a maximum tryptophan–heme separation of 43 ± 2 Å occurs for $K^2 = 4$, its maximum value. Thus, from this analysis the heme moiety is at most about 25 Å from the surface of the bilayer.

AO–Heme Energy Transfer. Energy transfer between the AO probes and the heme of whole cytochrome was determined by measuring the quenching of AO fluorescence upon addition of whole protein to vesicles (NPP had no effect). The R_0 values were determined for AO fluorescence in vesicles and were found to be about 38 Å (Table II), in good agreement with the results for hemoglobin (Shaklai et al., 1977; Eisinger & Flores, 1982). The quenching of AO fluorescence was analyzed for three heme densities (protein concentrations), and the results are shown in Figure 7. The Z_A variation of T exhibited in Figure 7 reflects both the variation in R_0 and the heme–AO separation (R_{HA}). Thus, T is relatively independent of probe position since both R_{HA} and R_0 tend to increase with depth. Although the uncertainties are fairly large, we can use these results to place limits on the range of possible heme positions. The expected transfer patterns for heme located at several positions along the central axis ($y = 0$) of the protein are shown in Figure 7. The calculated curves are most consistent with a heme position between 10 and 25 Å from the surface, in reasonable agreement with the tryptophan results.

Discussion

This study has demonstrated that energy transfer between tryptophan of membrane proteins and AO fatty acids follows the behavior expected from the model detailed in the previous paper (Kleinfeld, 1985). The membrane properties of the AO probes are critical parameters in the theory, and the most important of these are the Z_A values. Our finding that the tryptophan is located at 20 Å from the surface of the membrane, in agreement with the study of Fleming et al. (1979) and with predictions based on the primary sequence and secondary structure (Fleming et al., 1978; Dailey & Strittmatter, 1978), represents strong evidence in support of the assignment of Z_A positions. A uniform shift of all these positions would shift the position of the tryptophan by about the same amount. A shift of any individual probe in the 2–9-position by 3 Å would change T by between 10 and 20%. Since the b_5 tryptophan has considerable orientational freedom [cone angle > 30° (Fleming et al., 1979)], 3 Å probably represents the Z_A uncertainty for these probes. Although the positions of the deeper lying probes cannot be determined with similar accuracy from the results of the present study, evidence from previous studies (Podo & Blaisie, 1977; Lesslauer et al., 1972; Eisinger & Flores, 1982; Chalpin & Kleinfeld, 1983) together with our results suggests that the adopted AO positions are accurate to about 3 Å. This study does not lend itself to the determination of the sign of Z_A since the tryptophan

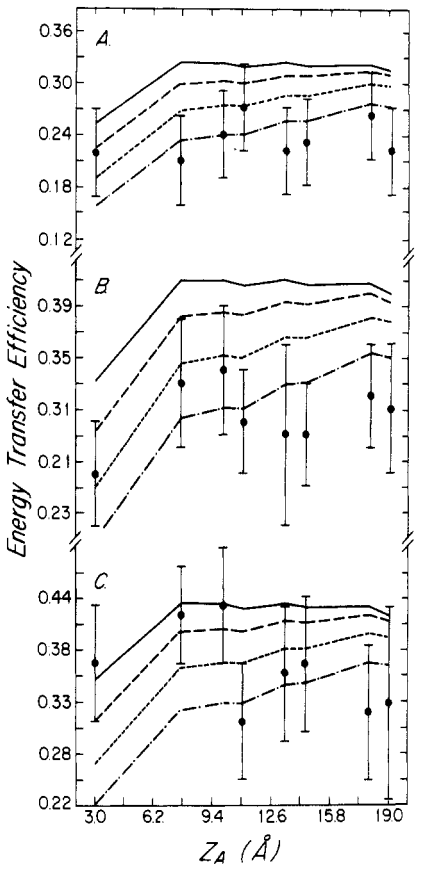

FIGURE 7: Energy transfer from AO to the heme of cytochrome b_5. Energy-transfer efficiencies were determined from the quenching of AO fluorescence, as described in the text. These values were determined, for a fixed protein concentration, by averaging the efficiencies from several different AO probe densities, since the efficiency is independent of donor concentration. The uncertainties are standard deviations about the average. The curves are the expected pattern calculated with the heme acceptor along the central axis of the protein ($y = 0$) and at several different z positions (in Å): (—) 25, (- - -) 30, (···) 35, and (-·-) 40. The results are for three different protein concentrations (in pmol/cm^2): A = 1.8, B = 2.5, and C = 2.7.

is at the center of the bilayer. The heme transfer efficiencies are also not sensitive enough for this purpose because of large experimental uncertainties and R_0 values.

These AO positions are averages since the molecule undergoes rotations and translations. Virtually all studies of the AO properties in membrane demonstrate that the individual probes sample different environments and that this variation with probe position varies monotonically with AO position (Podo & Blasie, 1977; Lesslauer et al., 1972; Thulborn & Sawyer, 1978; Eisinger & Flores, 1982; Vincent et al., 1982; Chalpin & Kleinfeld, 1983). This suggests that the width of the z-position distribution must be less than about 3 Å, and therefore, it is valid to use these positions to calculate T.

The model assumption of a uniform lateral distribution is *consistent* with our finding that the same protein structure is obtained at all probe densities. It is possible to estimate the degree of probe uniformity from measurements of the concentration quenching of fluorescence polarization of the AO probes (Snyder & Freire, 1982). Measurements in both egg PC vesicles and red cell ghosts indicate that the probes are uniformly distributed (A. Kleinfeld, unpublished observations).

Förster energy transfer in the general case of a single donor acceptor pair is a sensitive function of K^2 (Dale et al., 1979). Measurements of decay anisotropy in liposomes above and below the phase transition temperature (Vincent et al., 1982, Kutchai et al., 1983) and our own studies in egg PC and red

Table III: Coordinates (in Angstroms) Determined from Energy-Transfer Measurements[a]

	radial parameter	Y_{Trp}	Z_{Trp}	Z_{heme}
NPP	14 ± 2	8 ± 3	−1 ± 3	
whole b_5	18 ± 2	10 ± 3	1 ± 3	35 ± 5

[a] The uncertainties are standard deviations obtained from multiple determinations.

cell ghosts (Kleinfeld, unpublished observations) demonstrate that there is little or no restriction to the rapid rotational mobility of the probes in membranes. Taken together with the mixed dipole character of the AO absorption band (Matayoshi & Kleinfeld, 1981), where it overlaps tryptophan emission, these results suggest that the model of an isotropic distribution of AO dipoles, discussed in the previous paper (Kleinfeld, 1985), is appropriate in the present case. Hence, we expect the uncertainty in the tryptophan or heme orientation to have little affect on the analysis. This is especially true in the case of cytochrome b_5, which has considerable tryptophan rotational freedom (Fleming et al., 1979; Markelo and Holloway, private communication).

Another source of uncertainty in the analysis is the choice of index of refraction of the medium between the donor and acceptor. Little is known about the polarizability of the environment around tryptophan in proteins. In the case of b_5, however, the surrounding medium is probably characteristic of long-chain hydrocarbons ($n = 1.4$). Since various bilayer properties such as polarity and density decrease with depth, n probably also varies with position in the bilayer. We have calculated the transfer efficiencies with two models for the depth variation of n. In the first we assumed that n was constant and equal to 1.4. In the second, the values of n measured in solvent systems of various polarities and densities were surveyed to match those that might exist in the bilayer. This yielded an empirical expression in which n varied linearly between 1.38 and 1.5 ($n = 1.38 + 0.003Z_A$) for between the 2- and the 18-position, respectively. The tryptophan position obtained with the Monte Carlo analysis using either scheme varied by less than 2 Å. We have therefore adopted the values obtained with the empirical expression.

Although we have used the agreement between our results and those of Fleming et al. (1979) to verify the method of analysis, none of the parameters used in the model were determined from the cytochrome b_5 results. It is reasonable, therefore, to use the present study to extract information about the structure of b_5. Our results and those of Fleming et al. (1979) indicate that the tryptophan position is similar in whole protein and NPP (Table III). This suggests that the hydrophobic portion is not anchored by the hydrophilic segment. Furthermore, the midplane location of the tryptophan implies that the configuration of the membrane-bound portion of the protein must be either a hairpin loop or a single transbilayer segment with the 109 residue at the center. In the latter case it is difficult to understand why the C terminus with two net negative charges should penetrate the bilayer, while the N terminus with only a single net positive charge should not. A loop arrangement of this kind may be quite general for membrane proteins that have only a single hydrophobic domain and are exogenously inserted into the bilayer (Cardoza et al., 1984).

The radial parameter determined in this study is the distance between the central axis of the protein and the center of the AO probe. As indicated in Figure 8 the relationship of this parameter to the protein dimensions depends on what factors limit the distance of closest approach of the AO probe: the

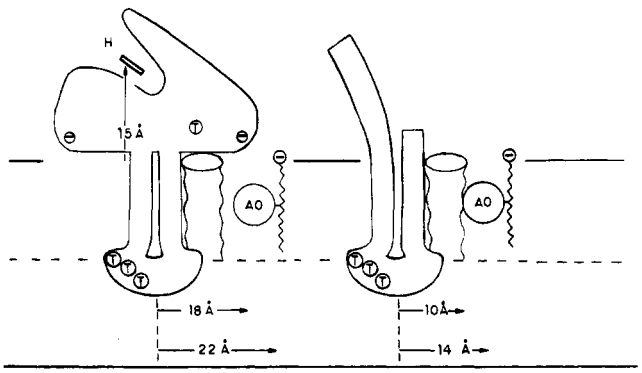

FIGURE 8: Model of whole cytochrome b_5 and NPP. The model of Dailey & Strittmatter (1981) has been extended to incorporate the results of the present study. The whole protein is shown on the left and NPP on the right. Also shown is the tightly bound lipid molecule, suggested by Fleming & Strittmatter (1978), and an AO probe at the distance of closest approach for each peptide. The models have been drawn approximately to scale by using a projection of the hydrophilic segment determined by X-ray diffraction (Mathews et al., 1979) and the β and helical structure of the NPP segment (Dailey & Strittmatter, 1981). The center of the heme moiety has been placed in an aqueous pocket 15 Å from the surface of the membrane, as suggested by the X-ray diffraction results (Mathews et al., 1979) and the present study.

carboxyl terminus or the AO moiety. Since either configuration is consistent with the energy-transfer results, other considerations must be invoked to obtain information about protein dimensions. On the basis of CD measurements and a Chou–Fasman interpretation of the primary sequence, Dailey & Strittmatter (1981) argued that the hydrophobic portion of the protein is formed by a stalk, consisting of two antiparallel β sheets, joined at the midplane of the bilayer by a loop of β-turn and α-helical structures. A cylinder enclosing the two β sheets has a radius of about 5 Å.

For NPP we obtained a radial parameter of 14 Å, which if we take the probe radius as 4 Å, suggests an effective protein radius of 10 ± 2 Å or 18 ± 2 Å, for restriction due to the probe or C terminus, respectively. Clearly neither is compatible with a bare protein. Fleming & Strittmatter (1978), however, have suggested that the protein is surrounded by seven to eight lipid molecules which, if these were tightly bound, might serve as a barrier to the AO probes. If the diameter of a lipid molecule is taken to be 8 Å, the radius of a cylinder formed by the protein plus a single lipid shell is about 13 Å. Since this is in better agreement with the value 10 ± 2 than 18 ± 2 Å, it is likely that the internal portion of the protein plus an annulus of lipid limits the lateral distribution of the probe.

Our results suggest that the effective protein radius may be somewhat greater in whole b_5 than NPP. Since the tryptophan position is the same in both structures and the hydrophilic segment probably does not extend into the membrane, this increase in effective size is probably due to an interaction between the protein and the carboxyl terminus of the probe. This suggests that the effective protein radius of the hydrophilic segment is about 22 ± 2 Å. Although it is not clear if the bulk of the hydrophilic segment could spread out on the membrane surface to create a barrier of this radius [the long dimension is 40 Å (Mathews et al., 1979)], this part of the protein is anionic and might, therefore, generate an electrostatic barrier for the negatively charged AO probes. In this regard it is interesting that Fleming et al. (1979) suggested that such a repulsion significantly increased the effective radius for the negatively charged probe used in their study, (trinitrophenyl)phosphatidylethanolamine, as compared to the neutral dansyldodecylamine. In their study, however, the radius was found to be 16 Å compared to our value of 22 Å.

The results of the present study represent the first determination of the heme position for the membrane-bound protein. Energy transfer from tryptophan and the AO probes suggests that the heme moiety is about 15 Å from the surface of the membrane. According to Mathews et al. (1979) the heme is located in what is probably an aqueous pocket in the hydrophilic portion of the protein located about 30 Å from one end of the molecule. Since the heme is near the edge of the pocket and since we expect the hydrophilic portion to abut the membrane in order to form the barrier for the probes, it is unlikely that the pocket faces the membrane surface. The constraints of the crystallographic work and the heme–membrane distance also indicate that the pocket cannot be vertical. A configuration consistent with these constraints must have the heme pocket inclined from the vertical, approximately as shown in Figure 8. In this configuration the heme moiety may be in an advantageous position to serve in its electron-transfer function.

ACKNOWLEDGMENTS

We would like to thank Dr. Peter Holloway for his generous gift of cytochrome b_5.

Registry No. b_5, 9035-39-6; DMPC, 13699-48-4; Trp, 73-22-3; 2-AS, 78447-89-9; 3-AS, 86637-08-3; 6-AS, 67708-95-6; 7-AS, 78447-90-2; 9-AS, 69243-44-3; 10-AS, 56970-51-5; 12-AS, 30536-60-8; 16-AP, 64821-29-0; heme, 14875-96-8.

REFERENCES

Cardoza, J. D., Kleinfeld, A. M., Stallcup, K. C., & Mescher, M. F. (1984) *Biochemistry 23*, 4401–4409.

Chalpin, D. B., & Kleinfeld, A. M. (1983) *Biochim. Biophys. Acta 731*, 465–474.

Dailey, H. A., & Strittmatter, P. (1981) *J. Biol. Chem. 256*, 3951–3955.

Dale, R. E., Eisinger, J., & Blumberg, W. E. (1979) *Biophys. J. 26*, 161–193.

Eisinger, J. (1969) *Photochem. Photobiol. 9*, 247–258.

Eisinger, J., & Flores, J. (1982) *Biophys. J. 37*, 6–7.

Fleming, P. J., & Strittmatter, P. (1978) *J. Biol. Chem. 253*, 8198–8202.

Fleming, P. J., Dailey, H. A., Corcoran, D., & Strittmatter, P. (1978) *J. Biol. Chem. 253*, 5369–5372.

Fleming, P. J., Koppel, D. E., Lau, A. L. Y., & Strittmatter, P. (1979) *Biochemistry 18*, 5458–5464.

Gomori, G. (1942) *J. Lab. Clin. Med. 27*, 955–960.

Haigh, E. A., Thulborn, K. R., & Sawyer, W. H. (1979) *Biochemistry 18*, 3525–3532.

Huang, C., & Mason, J. T. (1978) *Proc. Natl. Acad. Sci U.S.A. 75*, 308–310.

Kleinfeld, A. M. (1985) *Biochemistry* (previous paper in this issue).

Kleinfeld, A. M., Pandiscio, A. A., & Solomon, A. K. (1979) *Anal. Biochem. 94*, 65–74.

Kutchai, H., Chandler, L. H., & Zavoico, G. B. (1983) *Biochim. Biophys. Acta 736*, 137–149.

Lesslauer, W., Cain, J. E., & Blasie, J. K. (1972) *Proc. Natl. Acad. Sci. U.S.A. 69*, 1499–1503.

Leto, T. L., & Holloway, P. W. (1979) *J. Biol. Chem. 254*, 5015–5019.

Matayoshi, E. D., & Kleinfeld, A. M. (1981) *Biophys. J. 35*, 215–235.

Mathews, F. S., Czerwinski, E. W., & Argos, P. (1979) in *The Porphyrins* (Dolphin, D., Ed.) Vol. III, pp 107–145, Academic Press, New York.

Podo, F., & Blasie, J. K. (1977) *Proc. Natl. Acad. Sci. U.S.A. 74*, 1032–1036.
Scott, T. G., Spencer, R. D., Leonard, N. J., & Weber, G. (1970) *J. Am. Chem. Soc. 92*, 687–695.
Shaklai, N. Yguerabide, J., & Ranney, H. M. (1977) *Biochemistry 16*, 5585–5592.
Shinitzky, M. (1972) *J. Chem. Phys. 56*, 5979–5981.
Snyder, B., & Freire, E. (1982) *Biophys. J. 40*, 137–148.
Thulborn, K. R., & Sawyer, W. H. (1978) *Biochim. Biophys. Acta 511*, 125–140.
Vincent, M., Forest, B., Gallay, J., & Alfsen, A. (1982) *Biochemistry 21*, 708–716.

High-Resolution Cross-Polarization/Magic Angle Spinning ^{13}C NMR of Intracytoplasmic Membrane and Light-Harvesting Bacteriochlorophyll–Protein of Photosynthetic Bacteria†

Tsunenori Nozawa,* Mitsushi Nishimura, and Masahiro Hatano
Chemical Research Institute of Non-aqueous Solutions, Tohoku University, Sendai 980, Japan
Hidenori Hayashi
Department of Chemistry, Faculty of Science, The University of Tokyo, Bunkyo-ku, Tokyo 113, Japan
Keizo Shimada
Department of Biology, Faculty of Science, Tokyo Metropolitan University, Fukazawa, Setagaya-ku, Tokyo 158, Japan
Received July 2, 1984

ABSTRACT: Solid-state ^{13}C NMR spectra of intracytoplasmic membrane (ICM) and light-harvesting bacteriochlorophyll–protein complex 2 (LH2) of *Rhodopseudomonas palustris* were observed first at 75.46 MHz (under a 7.05 T static magnetic field) by a high-power decoupling, cross-polarization and magic angle spinning (MAS) methods in conjunction with total elimination of spinning side band techniques. At the MAS rate of 3300 Hz, ICM and LH2 yielded ^{13}C NMR spectra with high resolution. The variation of contact times yields selected NMR spectra which are mostly attributed to the proteins, lipids, and bacteriochlorophyll *a*, respectively. Further, the relaxation rates for resolved resonances were determined, and the dynamic behavior of the lipid, protein, and bacteriochlorophyll *a* was discussed in terms of the estimated relaxation rates.

The photosynthetic apparatus of the photoheterotrophic bacterium *Rhodopseudomonas palustris* is localized in a system of intracytoplasmic membrane (ICM)[1] (Cohen-Bazire & Sistrom, 1966) which, upon mechanical disruption, gives rise to small membrane vesicles occasionally called "chromatophores" (Niederman & Gibson, 1978). ICM contains most of the light-harvesting (LH) and reaction center bacteriochlorophyll (BChl) *a*–protein complexes (Niederman & Gibson, 1978). Absorption spectra revealed that these LH complexes are composed of several components designated as B870, B850, and B800 on the basis of their absorption maxima in the near-infrared (Sistrom, 1964). Two types of LH–BChl–proteins have been isolated from chromatophores of *Rps. palustris*. These were designated as LH1 and LH2. LH1 is the LH–BChl–protein that includes B870, and LH2 is the one that contains B850 and B800 (Hayashi et al., 1982a–c).

Because of high molecular weights and restricted molecular motions, the BChl–proteins in solution could not give high-resolution ^{13}C NMR signals by the conventional FT NMR method for low molecular weight compounds in solutions. Hence, the use of NMR for the photosynthetic system had been limited. However, the solid-state high-resolution NMR techniques have emerged as a powerful method to obtain high-resolution ^{13}C NMR spectra of solid samples (such as ICM and BChl–proteins) which allow us to discuss dynamic structures of the photosynthetic system in situ.

In general the effects of ^{1}H–^{13}C magnetic dipole–dipole interactions, ^{13}C chemical shift anisotropies, and the time bottleneck of long ^{13}C spin–lattice relaxation times render the direct application of the liquid-state ^{13}C NMR technique to solid samples essentially useless, yielding broad and featureless spectra of low intensity. Pines et al. introduced the technique of high-power ^{1}H decoupling for eliminating the broadening effect of ^{1}H–^{13}C dipolar interactions, with ^{13}C–^{1}H cross-polarization (CP) to circumvent the ^{13}C–T_1 bottleneck (Pines et al., 1973). Schaefer & Stejskal (1976) then introduced the use of magic angle spinning (MAS) to average out the ^{13}C chemical shift anisotropy (Andrew, 1971) and demonstrated that the CP/MAS combination provides a powerful technique that is capable of yielding high-resolution ^{13}C NMR spectra of solid samples.

In this paper we will report a benefit of the application of the solid-state ^{13}C NMR (called CP/MAS NMR) to some complex biomolecular systems (ICM and LH proteins). Since the resolution was high enough to identify each carbon resonance, the dynamic structures of the constituents, i.e., protein, BChl *a*, and lipid, could be explored. Recently ^{13}C CP/MAS NMR spectra have been reported on chlorophyll *a* (Brown et

† This work was supported in part by a Grant-in-Aid for Scientific Research from the Ministry of Education, Science and Culture, Japan, and by a grant from Nissan Science Foundation to M.H.

[1] Abbreviations: CP, cross-polarization; ICM, intracytoplasmic membrane; LH, light harvesting; *Rps.*, *Rhodopseudomonas*; MAS, magic angle spinning; SDS, sodium dodecyl sulfate; NMR, nuclear magnetic resonance; Me_4Si, tetramethylsilane; TOSS, total elimination of spinning side bands; FT, Fourier transform.

0006-2960/85/0424-1890$01.50/0